Spin Nematic State as a Candidate of the Hidden Order Phase of URu_2Si_2

Satoshi Fujimoto

Department of Physics, Kyoto University, Kyoto 606-8502, Japan
(Received 28 January 2011; revised manuscript received 6 April 2011; published 13 May 2011)

Motivated by the recent discovery of broken fourfold symmetry in the hidden order phase of URu_2Si_2 [R. Okazaki *et al.*, Science **331**, 439 (2011)], we examine a scenario of a spin nematic state as a possible candidate of the hidden order phase. We demonstrate that the scenario naturally explains most of experimental observations, and furthermore, reproduces successfully the temperature dependence of the spin anisotropy detected by the above-mentioned experiment in a semiquantitative way. This result provides strong evidence for the realization of the spin nematic order.

DOI: 10.1103/PhysRevLett.106.196407 PACS numbers: 71.27.+a, 75.30.Mb

The heavy fermion compound URu_2Si_2 exhibits a second order phase transition at $T_{HO} \approx 17.5$ K. In spite of long-standing enormous efforts in experimental and theoretical studies [1–14], the order parameter of this phase transition has not yet been identified. The enigmatic features of this so-called "hidden order (HO)" phase are described as follows: (i) Despite the large anomaly in thermodynamic quantities and drastic reconstruction of the Fermi surfaces at $T = T_{HO}$, there is neither conventional magnetic order nor a change in the crystal structure [1–3,15–19]; (ii) however, under applied pressure, an antiferromagnetic (AF) state with a large moment appears, and more surprisingly, the Fermi surfaces in the AF ordered state are almost the same as those found in the HO phase [20–24].

Recently, an experimental breakthrough for this issue was achieved by Okazaki *et al.* [25], who found spontaneous symmetry breaking in the spin space at $T < T_{HO}$. They reported that the anisotropy of the spin susceptibility in the xy plane, which is measured by the quantity $\chi_{xy} = \langle S_x S_y \rangle$, becomes nonzero below T_{HO}. Since URu_2Si_2 is tetragonal with fourfold symmetry at $T > T_{HO}$, and the phase transition at $T = T_{HO}$ does not accompany any lattice distortion, it is reasonable to expect that this symmetry breaking is an essential feature of the HO phase, which imposes a crucial constraint on possible candidates of the HO parameter. Motivated by this experimental observation, in this Letter, we discuss a possibility that a spin nematic (SN) state is realized as the hidden order in URu_2Si_2. The SN phase is a state with circulating spin currents, but with no magnetic moment [26–28]. The circulating spin currents break spin rotational symmetry, leading to spin anisotropy, without breaking time-reversal symmetry. We demonstrate that the above-mentioned features of the HO phase are naturally understood within the scenario of the SN order, and furthermore, that the temperature dependence of the spin anisotropy spontaneously generated in the SN state successfully explains the above experimental observation in a semiquantitative way, providing strong evidence for the realization of the SN state as the HO phase of URu_2Si_2.

We, first, present a mean field analysis for basic properties of the SN state applied to the case of URu_2Si_2. The SN state is induced by nesting of the Fermi surface as discussed in Refs. [26,27]. In fact, the recent band calculations for URu_2Si_2 based on an itinerant f-electron picture revealed that there is one electron band denoted as $\varepsilon_{\boldsymbol{k}_1}$ and one hole band denoted as $\varepsilon_{\boldsymbol{k}_2}$ [22,29], which are nested to each other via the nesting vector $\boldsymbol{Q}_0 = (0, 0, \pi)$: i.e., $\varepsilon_{\boldsymbol{k}+\boldsymbol{Q}_0 1} = -\varepsilon_{\boldsymbol{k}2}$ [30,31]. It is noted that $\boldsymbol{Q}_0$ is equivalent to the ordering vector of the large-moment AF state which is observed under applied pressure [20]. Moreover, it was pointed out that several experimental results suggest that the energy gap opens on the Fermi surface below T_{HO} [18,32–35], which is consistent with the gap generation due to the nesting of the Fermi surface. Because of these reasons, we employ the scenario that itinerant f electrons undergo the transition to the SN state triggered by the Fermi surface nesting. We will discuss the microscopic origin of this instability later. Since the ordering vectors for the large-moment AF phase and the SN phase are the same, the feature (ii) mentioned above is naturally understood within our scenario. The SN phase is a spin-triplet electron-hole pairing state [26,27], and hence the order parameter of the SN state for the effective two-band model is

$$\mathcal{O}^{SN}_{\sigma\sigma'}(\boldsymbol{k}) = \langle c^\dagger_{\boldsymbol{k}1\sigma} c_{\boldsymbol{k}+\boldsymbol{Q}_0 2\sigma'} \rangle = \boldsymbol{d}_{12}(\boldsymbol{k}) \cdot \boldsymbol{\sigma}_{\sigma\sigma'}, \qquad (1)$$

where $c^\dagger_{\boldsymbol{k}a\sigma}$ ($c_{\boldsymbol{k}a\sigma}$) is a creation (an annihilation) operator for an electron in the band $a = 1, 2$ with momentum $\boldsymbol{k}$, spin σ. $\boldsymbol{d}_{12}(\boldsymbol{k})$ is a vector, the direction of which is parallel to the spin quantization axis of the SN order. Because of time-reversal invariance in the SN state, we have the condition $\boldsymbol{d}^*_{12}(-\boldsymbol{k}) = -\boldsymbol{d}_{12}(\boldsymbol{k})$. Furthermore, we impose inversion symmetry, since there is no indication of broken inversion symmetry in URu_2Si_2 from experiments. Then, it follows that $\boldsymbol{d}^*_{12}(\boldsymbol{k}) = -\boldsymbol{d}_{12}(\boldsymbol{k})$. Also, we assume that $\boldsymbol{d}_{ab}(\boldsymbol{k})$ is symmetric with respect to the exchange of the band indices a and b. This assumption will be plausibly justified by a microscopic argument given later. The mean field Hamiltonian for the SN state of the effective two-band model is $\mathcal{H}_{\rm MF} = \mathcal{H}^{(0)}_{\rm MF} + \mathcal{H}^{(1)}_{\rm MF}$ with the kinetic energy term $\mathcal{H}^{(0)}_{\rm MF} = \sum_{\boldsymbol{k},\sigma} \sum_{a=1,2} \varepsilon_{\boldsymbol{k}a} c^{\dagger}_{\boldsymbol{k}a\sigma} c_{\boldsymbol{k}a\sigma}$, and the particle-hole pairing term

$$\mathcal{H}^{(1)}_{\rm MF} = \sum_{\boldsymbol{k},\sigma,\sigma'} \sum_{\substack{a,b \\ a\neq b}} [\boldsymbol{d}_{ab}(\boldsymbol{k}) \cdot \boldsymbol{\sigma}_{\sigma\sigma'} c^{\dagger}_{\boldsymbol{k}+\boldsymbol{Q}_0 a\sigma} c_{\boldsymbol{k}b\sigma'} + \text{H.c.}]. \qquad (2)$$

For URu_2Si_2, the crystal structure of which has the D_{4h} symmetry, the anisotropy of the spin susceptibility which breaks fourfold symmetry down to twofold symmetry in the xy plane implies that the order parameter belongs to two-dimensional (2D) representation of the D_{4h} symmetry, and in the hidden order phase, fourfold symmetry in the 2D space is spontaneously broken. Then, from the symmetry properties of $\boldsymbol{d}_{12}(\boldsymbol{k})$ discussed above, a possible candidate is the E_g state with $\boldsymbol{d}_{12}(\boldsymbol{k}) = i(\Delta_1 k_y k_z, \Delta_2 k_x k_z, 0)$ [or $i(\Delta_1 k_x k_z, \Delta_2 k_y k_z, 0)$] for small $|\boldsymbol{k}|$. Here, the real parameters Δ_1 and Δ_2 are determined from the self-consistent gap equation.

According to the experiment [25], the axis of the Ising-like anisotropy, which is spontaneously generated in the HO phase, is parallel to the (1,1,0) direction. Since our toy model has continuous rotational symmetry in the xy plane, the analysis given here is applicable to URu_2Si_2 by rotating the principle axes by $\pi/4$ around the z axis, i.e., $x' = \frac{1}{\sqrt{2}} \times (x - y)$ and $y' = \frac{1}{\sqrt{2}}(x + y)$. Following the experimental observation, we assume that fourfold symmetry in the $x'y'$ plane is spontaneously broken, resulting in the state with $\boldsymbol{d}_{12}(\boldsymbol{k}) \parallel (1, 0, 0)$ or $(0, 1, 0)$ in this rotated spin frame. The direction of $\boldsymbol{d}_{12}(\boldsymbol{k})$ is determined by the detail of the electronic structure and spin-orbit interaction. However, most of the following results do not depend on it. For the tight-binding model, we choose

$$\boldsymbol{d}_{12}(\boldsymbol{k}) = (i\Delta_1 \phi(\boldsymbol{k}), 0, 0), \qquad \phi(\boldsymbol{k}) = \sin k_{\mu'} \sin k_z, \quad (3)$$

where $\mu' = x'$ or y'.

At this stage, we note that the electron-hole pairing term (2) is nonzero only when the nesting vector $\boldsymbol{Q}_0$ and the momentum dependence of $\boldsymbol{d}_{ab}(\boldsymbol{k})$ fulfill the following relation: $e^{-i\boldsymbol{Q}_0 \boldsymbol{r}_i} - e^{i\boldsymbol{Q}_0 \boldsymbol{r}_j} \neq 0$ for $\boldsymbol{r}_i$, $\boldsymbol{r}_j$ satisfying $\Delta_{ij} = \sum_{\boldsymbol{k}} \phi(\boldsymbol{k}) e^{-i\boldsymbol{k}(\boldsymbol{r}_i - \boldsymbol{r}_j)} \neq 0$. For (3) and $\boldsymbol{Q}_0 = (0, 0, \pi)$, this is actually fulfilled. It is instructive to compare this property of the SN phase with the unconventional spin density wave (USDW) state considered in Refs. [3,6], the order parameter of which is also given by Eq. (1) but with $\boldsymbol{d}_{12}$ a real even function of $\boldsymbol{k}$, because of broken time-reversal symmetry. It is easy to see that, if $\boldsymbol{Q}_0 = (0, 0, \pi)$, and the momentum dependence of $\boldsymbol{d}_{12}(\boldsymbol{k})$ is the same as (3), the particle-hole paring term (2) vanishes, and hence, this type of the USDW can not be realized. It is noted that the USDW is more stabilized than the SN phase, if the order parameter $\boldsymbol{d}_{ab}(\boldsymbol{k})$ (and hence, the particle-hole pairing interaction) is antisymmetric with respect to the exchange of the band indices a, b, or if higher harmonics of the order parameter such as $\phi(\boldsymbol{k}) = \sin 2k_{\mu'} \sin 2k_z$ is allowed.

We, now, calculate the anisotropy of the uniform spin susceptibility, which characterizes the SN order, and was experimentally detected in Ref. [25]. The anisotropy in the $x'y'$ plane for our model is obtained as $\Delta\chi(T) \equiv \chi_{y'y'}(T) - \chi_{x'x'}(T) = \mu_{\rm B}^2 \sum'_{\boldsymbol{k}} [\frac{\tanh\frac{E_{\boldsymbol{k}}}{2T}}{E_{\boldsymbol{k}}} - \frac{1}{2T\cosh^2\frac{E_{\boldsymbol{k}}}{2T}}] \frac{|\boldsymbol{d}_{12}(\boldsymbol{k})|^2}{4E^2_{\boldsymbol{k}}}$ where $E_{\boldsymbol{k}} = \sqrt{\varepsilon^2_{\boldsymbol{k}1} + |\boldsymbol{d}_{12}(\boldsymbol{k})|^2}$, and the momentum sum $\sum'_{\boldsymbol{k}}$ is taken over the nested part of the Fermi surface satisfying the condition $\varepsilon_{\boldsymbol{k}+\boldsymbol{Q}_0 1} = -\varepsilon_{\boldsymbol{k}2}$. Also, we assume the BCS mean-field-like T dependence of the amplitude of the gap $\Delta_1(T)$. To make a semiquantitative comparison with the experimental data without referring to the details of the band structure, we consider a ratio $\Delta\chi(T)/\Delta\chi(0)$, for which it is expected that effects of specific band structures approximately cancel out. There are two parameters in this calculation: one is the ratio of the energy gap at $T = 0$ to the transition temperature, i.e., $\Delta_1(0)/T_{\rm HO}$, and the other is an overall normalization factor of the magnitude. According to the recent scanning tunneling microscopy (STM) measurement, the magnitude of the gap opened on the Fermi surface via the hidden order transition is $\Delta_1(0) \sim 4$ meV [32,33]. Since $T_{\rm HO} = 17.5$ K, we choose the parameter as $\Delta_1(0)/T_{\rm HO} = 2.6$. Then, there is only one fitting parameter, i.e., the overall normalization factor. We choose the normalization factor to fit the theoretical result at $T = 6$ K to the experimental data at the same temperature. The calculated result of this one-parameter fitting is shown in Fig. 1(a). In spite of simplicity of the model, the theoretical result is surprisingly in good agreement with the experimental observations, at least above $T/T_{\rm HO} \sim 0.15$. A slight discrepancy at low temperatures may be ascribed to the superconducting transition. This result provides strong evidence for the realization of the SN state as the HO in URu_2Si_2. In Fig. 1(a), the T-linear behavior of $\Delta\chi(T)$ at low temperatures is seen, which is raised by the existence of the line node of the order parameter (3). The experimental data are also consistent with this behavior above $T/T_{\rm HO} \sim 0.15$.

The above scenario also has important implications for magnetic properties of the HO phase. According to neutron scattering measurements, there is a longitudinal spin fluctuation with the wave number $\boldsymbol{q} = \boldsymbol{Q}_0$, which exhibits an excitation gap in the HO phase [34]. Remarkably, the magnitude of the spin gap $\sim$1.6 meV is much smaller than the single particle energy gap $\Delta_1 \sim 4$ meV observed via the STM measurements [32,33]. Furthermore, the spin gap increases notably with increasing a magnetic field applied along the z axis, H_z;, e.g., the spin gap for $H_z = 17$ T reaches to 2.5 meV [34]. These properties are well explained by the present model. Using the mean field Hamiltonian $\mathcal{H}_{\rm MF}$ and the random phase approximation,

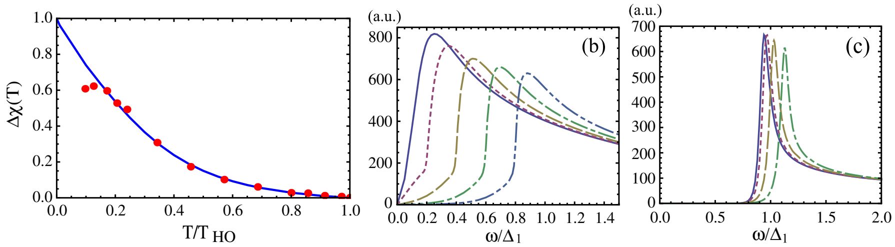

FIG. 1 (color online). (a) Solid line: anisotropy of the spin susceptibility $\Delta\chi = \chi_{x'x'} - \chi_{y'y'}$ in the SN phase versus T/T_{HO}. The magnitude of $\Delta\chi$ is normalized by the value at $T = 0$. Circle: experimental data quoted from [25]. $\Delta_1(0)/T_{\mathrm{HO}} = 2.6$. (b) $\mathrm{Im}\chi^{zz}(\boldsymbol{Q}_0, \omega)$ versus ω/Δ_1. $\mu_{\mathrm{B}}H_z/\Delta_1 = 0$ (solid), 0.1 (dotted), 0.2 (dashed), 0.3 (dot-dashed), 0.4 (double-dot-dashed). (c) $\mathrm{Im}\chi^{zz}(\boldsymbol{Q}_1, \omega)$ versus ω/Δ_1. $\mu_{\mathrm{B}}H_z/\Delta_1 = 0$ (solid), 0.1 (dotted), 0.2 (dashed), 0.3 (dot-dashed).

we calculate the longitudinal spin correlation function $\chi^{zz}(\boldsymbol{q}, \omega) = -i\int_0^\infty dt \langle [S^z(\boldsymbol{q}, t), S^z(-\boldsymbol{q}, 0)]\rangle e^{i\omega t}$ for $\boldsymbol{q} = \boldsymbol{Q}_0$, which is dominated by the transition between the band $\varepsilon_{\boldsymbol{k}1}$ and the band $\varepsilon_{\boldsymbol{k}2}$ [36]. In Fig. 1(b), the imaginary part of $\chi^{zz}(\boldsymbol{Q}_0, \omega)$ is plotted as a function of the frequency ω/Δ_1, which indicates the spin excitation gap smaller than the single-electron gap Δ_1. As the magnetic field H_z increases, the excitation gap increases substantially. These behaviors are understood as a result of the existence of line nodes of the gap $|\boldsymbol{d}_{12}(\boldsymbol{k})|$. The line nodes allow low-energy spin excitations to develop below Δ_1. When the system is in the vicinity of magnetic criticality, a gap structure appears for $\omega < \Delta_1$, which is also sensitive to applied magnetic fields, as shown in Fig. 1(b). These results are in good agreement with the experimental observation obtained in Ref. [34]. Conversely, these neutron scattering data strongly imply the existence of line nodes in the energy gap. On the other hand, these experiments also revealed that in addition to $\boldsymbol{Q}_0$, there is a longitudinal incommensurate spin fluctuations with $\boldsymbol{Q}_1 = (1.4\pi, 0, 0)$ [15], which may be attributed to the nesting between the hole band $\varepsilon_{\boldsymbol{k}2}$ and another hole band denoted as $\varepsilon_{\boldsymbol{k}3}$, as suggested from the band calculations [22,30]. According to the recent experiments, the magnetic excitation for the incommensurate $\boldsymbol{Q}_1$ has an energy gap $\sim$4 meV below T_{HO} [18,34,37]. In our scenario, the gap $\sim$4 meV opens in the hole band $\varepsilon_{\boldsymbol{k}2}$ in the SN state, while it does not in the hole band $\varepsilon_{\boldsymbol{k}3}$. Thus, the magnetic excitations due to the transition between these two hole bands should exhibit the excitation energy gap $\sim$4 meV at the wave vector $\boldsymbol{Q}_1$ rather than 2×4 meV. This explains the above-mentioned experimental result. To demonstrate this, we calculate the spin correlation function $\chi^{zz}(\boldsymbol{Q}_1, \omega)$ for the mean field Hamiltonian [36]. In this calculation, we postulate that hot spots on the hole band 2 for this spin fluctuation are located away from the gap node of $|\boldsymbol{d}_{12}(\boldsymbol{k})|$; i.e., $|\boldsymbol{d}_{12}(\boldsymbol{k})| \neq 0$ for $\boldsymbol{k}$ satisfying $\varepsilon_{\boldsymbol{k}+\boldsymbol{Q}_1 2} \approx -\varepsilon_{\boldsymbol{k}3}$. Then, the sharp gap edge appears at $\omega = \Delta_1$ in $\mathrm{Im}\chi^{zz}(\boldsymbol{Q}_1, \omega)$, as shown in Fig. 1(c). In the case with magnetic fields H_z, the gap edge shifts to $\omega \approx \Delta_1 + 2H_z^2/\Delta_1$ [36]. Thus, the field dependence of $\mathrm{Im}\chi^{zz}(\boldsymbol{Q}_1, \omega)$ is much weaker than that of $\mathrm{Im}\chi^{zz}(\boldsymbol{Q}_0, \omega)$ [Fig. 1(c)]. This is also qualitatively in agreement with the experimental results [34,37].

Some remarks are in order: (i) In the SN state, there are staggered circulating spin currents [26,27]. When a uniform magnetic field parallel to (1, 1, 0) or (1, −1, 0) in the original frame is applied, and electron spins are polarized, the spin currents lead to the staggered orbital currents, which induce staggered moment, as in the case of the orbital current state [7]. In NMR experiments, broadening of spectra under applied fields was observed [16,17]. Its origin may be attributed to the staggered circulating currents of the SN state. The magnitude of the induced staggered field raised by the circulating currents is estimated as $\sim$1 Oe for the applied field $H \sim 4$ T, which is consistent with the experimental results [17]. (ii) Note that the USDW state with the spin quantization axis parallel to $(1, \pm1, 0)$ also exhibits the same spin anisotropy as the SN state, and may explain the experimental data of Ref. [25]. At this stage, we cannot thoroughly exclude the possibility of the USDW as a candidate of the HO, though, as mentioned before, the particle-hole pairing interaction antisymmetric with respect to the band indices, the origin of which is microscopically unclear, is required for its realization. (iii) The SN order parameter couples to a magnetic field $\boldsymbol{H}$ as $\sim(\boldsymbol{d}_{12} \cdot \boldsymbol{H})^2$ in the free energy. This implies that the nonlinear susceptibility χ_3 for a magnetic field $\boldsymbol{H}$ satisfying $\boldsymbol{d}_{12} \cdot \boldsymbol{H} \neq 0$ exhibits a discontinuous jump at $T = T_{\mathrm{HO}}$ for the SN order (3). However, such an anomaly was experimentally observed not for the in-plane field, but for the $\boldsymbol{H} \parallel z$ axis [3]. The discontinuous jump for the $\boldsymbol{H} \parallel z$ axis may be explained by postulating that the SN vector $\boldsymbol{d}_{12}$ is not confined in the xy plane, but rather has a nonzero out-of-plane component. This scenario may also explain the change of the slope of the linear spin susceptibility at $T = T_{\mathrm{HO}}$ for the $\boldsymbol{H} \parallel z$ axis. However, the absence of the jump for the in-plane field in the experiment remains to be resolved. It is desirable to reexamine the measurement of the nonlinear susceptibility using recent high-quality samples. (iv) According to specific heat measurements in magnetic fields parallel to the z-axis H_z, the specific heat jump ΔC at $T = T_{\mathrm{HO}}$ is almost constant as a function of H_z, though the transition temperature decreases as $T_{\mathrm{HO}}(H_z) - T_{\mathrm{HO}}(0) \propto -H_z^2$ [38,39]. These behaviors are explained by the SN scenario. The decrease of T_{HO} is understood as a result of the decrease of the particle-hole pairing interaction due to the magnetic field [36]. Also, the absence of the change of ΔC under applied fields is explained by taking into account the self-energy correction arising from interactions with AF spin fluctuations [36]. Within this scenario, the specific heat jump is given by $\Delta C \sim \xi^2 T_{\rm HO}$, where ξ is the correlation length for AF spin fluctuations. If the system is in the vicinity of the AF critical point, i.e., $\xi^2 \sim 1/T$, ΔC is constant, though $T_{\rm HO}$ is decreased by the magnetic field. (v) Experimental studies reported that under applied pressure, the discontinuous phase transition from the HO state to the large-moment AF state occurs [20], while the Fermi surfaces in both phases are almost the same [19,21,23,24]. According to our scenario, there are competing AF spin fluctuations and fluctuations toward the SN phase transition in the system (see below and supplemental material [36] for details). Thus, applied pressure induces the change of effective couplings between electrons and these fluctuations, resulting in the transition to the AF phase. Since the order parameters of these phases have the different symmetries that are not compatible with continuous phase transition, the type of the phase transition is first order, which is in agreement with experiments [17,20]. We stress that the reconstructed Fermi surfaces in the SN phase and the AF phase are the same in our scenario, because both of them are reconstructed by the same nesting vector $\boldsymbol{Q}_0$. This is also in agreement with experimental observations [19,21–24].

Finally, we discuss microscopic mechanism of the SN order for $\mathrm{URu_2Si_2}$ [36]. We consider a scenario that orbital fluctuations associated with the Fermi surface nesting yields the SN order. The minimal model consists of the three bands $\varepsilon_{\boldsymbol{k}a}$ with $a = 1, 2, 3$, and mutual Coulomb interaction between electrons. The SN order considered here arises from the particle-hole pairings in the d-wave channel which are formed between the electron band 1 and the hole band 2. The Fermi surface nesting with the nesting vector $\boldsymbol{Q}_0$ between these bands leads to this instability. An effective pairing interaction in the $d_{\mu' z}$-wave channel is mediated via orbital fluctuations arising from the Fermi surface nesting between $\varepsilon_{\boldsymbol{k}3(1)}$ and $\varepsilon_{\boldsymbol{k}2}$ with the nesting vector $\boldsymbol{Q}_1$ ($\boldsymbol{Q}_0$). If the orbital fluctuations are sufficiently strong, the SN order is stabilized [36].

In conclusion, we have demonstrated that the SN state induced by the Fermi surface nesting is a promising candidate of the HO phase of $\mathrm{URu_2Si_2}$, since it successfully explains most of the experimental observations including the recent experiment on fourfold symmetry breaking.

The author thanks Y. Matsuda and T. Shibauchi for invaluable discussions, and kindly providing the author with their experimental data. He is also indebted to A. V. Balatsky, P. M. Oppeneer, and A. Yazdani for useful discussions. This work is supported by the Grant-in-Aids for Scientific Research from MEXT of Japan (Grants No. 19052003 and No. 21102510).

[1] T. T. M. Palstra et al., Phys. Rev. Lett. **55**, 2727 (1985).
[2] M. B. Maple et al., Phys. Rev. Lett. **56**, 185 (1986).
[3] A. P. Ramirez et al., Phys. Rev. Lett. **68**, 2680 (1992).
[4] V. Barzykin and L. P. Gor'kov, Phys. Rev. Lett. **70**, 2479 (1993).
[5] P. Santini and G. Amoretti, Phys. Rev. Lett. **73**, 1027 (1994).
[6] H. Ikeda and Y. Ohashi, Phys. Rev. Lett. **81**, 3723 (1998).
[7] P. Chandra et al., Nature (London) **417**, 831 (2002).
[8] V. P. Mineev and M. E. Zhitomirsky, Phys. Rev. B **72**, 014432 (2005).
[9] A. Kiss and P. Fazekas, Phys. Rev. B **71**, 054415 (2005).
[10] C. M. Varma and L. Zhu, Phys. Rev. Lett. **96**, 036405 (2006).
[11] F. Cricchio et al., Phys. Rev. Lett. **103**, 107202 (2009).
[12] K. Haule and G. Kotliar, Nature Phys. **5**, 796 (2009).
[13] H. Harima, K. Miyake, and J. Flouquet, J. Phys. Soc. Jpn. **79**, 033705 (2010).
[14] Y. Dubi and A. V. Balatsky, Phys. Rev. Lett. **106**, 086401 (2011).
[15] C. Broholm et al., Phys. Rev. B **43**, 12 809 (1991).
[16] K. Matsuda et al., Phys. Rev. Lett. **87**, 087203 (2001).
[17] S. Takagi et al., J. Phys. Soc. Jpn. **76**, 033708 (2007).
[18] C. R. Wiebe et al., Nature Phys. **3**, 96 (2007).
[19] Y. J. Jo et al., Phys. Rev. Lett. **98**, 166404 (2007).
[20] H. Amitsuka et al., J. Magn. Magn. Mater. **310**, 214 (2007).
[21] M. Nakashima et al., J. Phys. Condens. Matter **15**, S2011 (2003).
[22] S. Elgazzar et al., Nature Mater. **8**, 337 (2009).
[23] E. Hassinger et al., Phys. Rev. Lett. **105**, 216409 (2010).
[24] R. Yoshida et al., Phys. Rev. B **82**, 205108 (2010).
[25] R. Okazaki et al., Science **331**, 439 (2011).
[26] H. J. Schulz, Phys. Rev. B **39**, 2940 (1989).
[27] A. A. Nersesyan, G. I. Japaridze, and I. G. Kimeridze, J. Phys. Condens. Matter **3**, 3353 (1991).
[28] The SN state considered here is different from the nematic state of $\mathrm{Sr_3Ru_2O_7}$ [see, e.g., E. Fradkin, S. A. Kivelson, M. J. Lawler, J. P. Eisenstein, and A. P. Mackenzie, Annu. Rev. Condens. Matter Phys. **1**, 153 (2010)] in that the former breaks rotational symmetry mainly in the spin space, while the latter breaks it in the momentum space, and that the former is raised by gap opening on the Fermi surface, while the latter is realized by the Pomeranchuk instability without gap formation.
[29] M. Biasini, J. Rusz, and A. P. Mills, Jr., Phys. Rev. B **79**, 085115 (2009).
[30] P. M. Oppeneer et al., Phys. Rev. B **82**, 205103 (2010).
[31] P. M. Oppeneer (private communication).
[32] P. Aynajian et al., Proc. Natl. Acad. Sci. U.S.A. **107**, 10 383 (2010).
[33] A. R. Schmidt et al., Nature (London) **465**, 570 (2010).
[34] F. Bourdarot et al., Phys. Rev. Lett. **90**, 067203 (2003).
[35] A. F. Santander-Syro et al., Nature Phys. **5**, 637 (2009).
[36] See supplemental material at http://link.aps.org/supplemental/10.1103/PhysRevLett.106.196407 for details.
[37] F. Bourdarot et al., J. Phys. Soc. Jpn. **79**, 064719 (2010).
[38] N. H. van Dijk et al., Phys. Rev. B **56**, 14493 (1997).
[39] M. Jaime et al., Phys. Rev. Lett. **89**, 287201 (2002).